Received: 9 December 2016 | Revised: 23 May 2017 | Accepted: 31 May 2017

DOI: 10.1111/cmi.12754

WILEY

RESEARCH ARTICLE

LC3-association with the parasitophorous vacuole membrane of *Plasmodium berghei* liver stages follows a noncanonical autophagy pathway

Rahel Wacker[1,2] | Nina Eickel[1,2] | Jacqueline Schmuckli-Maurer[1] | Takeshi Annoura[3] | Livia Niklaus[1,2] | Shahid M. Khan[4] | Jun-Lin Guan[5] | Volker T. Heussler[1]

[1] Institute of Cell Biology, University of Bern, Bern, Switzerland

[2] Graduate School for Cellular and Biomedical Sciences, University of Bern, Bern, Switzerland

[3] Department of Parasitology, National Institute of Infectious Diseases (NIID), Tokyo, Japan

[4] Center of Infectious Diseases, Leiden University Medical Center, Leiden, The Netherlands

[5] Department of Cancer Biology, University of Cincinnati College of Medicine, Cincinnati, OH, USA

Correspondence
Volker T. Heussler, Institute of Cell Biology, University of Bern, Bern, Switzerland.
Email: heussler@izb.unibe.ch

Funding information
Swiss National Science Foundation, Grant/Award Number: 310030_159519 and 316030_145013; SystemsX, Grant/Award Number: 51RTPO_151032; Japan Society for the Promotion of Science, Grant/Award Number: GR16106

Summary

Eukaryotic cells can employ autophagy to defend themselves against invading pathogens. Upon infection by *Plasmodium berghei* sporozoites, the host hepatocyte targets the invader by labelling the parasitophorous vacuole membrane (PVM) with the autophagy marker protein LC3. Until now, it has not been clear whether LC3 recruitment to the PVM is mediated by fusion of autophagosomes or by direct incorporation. To distinguish between these possibilities, we knocked out genes that are essential for autophagosome formation and for direct LC3 incorporation into membranes. The CRISPR/Cas9 system was employed to generate host cell lines deficient for either FIP200, a member of the initiation complex for autophagosome formation, or ATG5, responsible for LC3 lipidation and incorporation of LC3 into membranes. Infection of these knockout cell lines with *P. berghei* sporozoites revealed that LC3 recruitment to the PVM indeed depends on functional ATG5 and the elongation machinery, but not on FIP200 and the initiation complex, suggesting a direct incorporation of LC3 into the PVM. Importantly, in *P. berghei*-infected *ATG5*$^{-/-}$ host cells, lysosomes still accumulated at the PVM, indicating that the recruitment of lysosomes follows an LC3-independent pathway.

1 | INTRODUCTION

Malaria, with more than 200 million estimated cases and more than 400 thousand deaths per year, remains one of the most devastating diseases worldwide (World Health Organization, 2015). Once *Plasmodium* sporozoites are injected by an infected female *Anopheles* mosquito during blood feeding, they migrate to the liver and infect hepatocytes by the formation of a parasitophorous vacuole (PV). Although the PV membrane (PVM) originates from invagination of the host cell plasma membrane, it is remodelled by the parasite upon infection (Spielmann, Montagna, Hecht, & Matuschewski, 2012). Inside the vacuole, the parasite starts its exoerythrocytic development by transforming into a multinuclear schizont that undergoes massive replication. Finally, several thousand erythrocyte-infective merozoites are formed and safely released into the blood within merosomes (Sturm et al., 2006). Within the hepatocyte, the *Plasmodium* parasite shows one of the fastest replication rates among eukaryotes, necessitating that massive amounts of nutrients are obtained from the host cell (Bano, Romano, Jayabalasingham, & Coppens, 2007). At the same time, the parasite needs to escape defence mechanisms of the host cell.

Rahel Wacker and Nina Eickel contributed equally to this work.

Macroautophagy, hereafter called autophagy, is a catabolic process that allows cells to degrade and recycle intracellular substrates. Under certain stress conditions, such as starvation, autophagy is induced to maintain homeostasis as it can provide nutrients for essential cellular processes. In addition to maintaining cellular homeostasis, cells can use selective autophagy to remove damaged or deleterious elements from the cytoplasm. Selective autophagy can also serve as a cellular antimicrobial defence against intracellular pathogens, a process called xenophagy (Deretic & Levine, 2009; Knodler & Celli, 2011; Levine, Mizushima, & Virgin, 2011; Mostowy, 2013). Starvation-induced and selective autophagy are both characterised by the formation of double membrane autophagosomes that sequester the autophagic cargo (Levine et al., 2011; Mizushima & Komatsu, 2011). In mammalian cells, starvation initiates autophagosome formation through mTORC1 (mammalian target of rapamycin complex 1) inhibition. This leads to activation of the initiation complex, including FAK family kinase-interacting protein of 200 kDa (FIP200), which subsequently regulates a class III phosphatidylinositol 3-kinase complex. Local formation of phosphatidylinositol 3-phosphate (PI(3)P) promotes phagophore formation (Figure 1). The elongation of the phagophore requires complex membrane dynamics, dependent on two ubiquitin-like conjugation systems. In the first, ATG12 (AuTophaGy-related 12) is conjugated to ATG5 by ATG7 and ATG10. In the second, ATG7 and ATG3 mediate the conjugation of cytosolic LC3-I (microtubule-associated protein 1 light chain 3) to phosphatidylethanolamine (PE), forming LC3-II, which is then incorporated into the autophagosomal membrane. Once formed, autophagosomes fuse with lysosomes, leading to the degradation of their contents. LC3 belongs to the mammalian family of yeast Atg8 homologues. Because of the difference in its localization upon induction of autophagy, LC3 is widely used as an autophagy marker (Kabeya et al., 2000; Mizushima, 2004).

Recently, it has been described that in *Plasmodium berghei*-infected hepatocytes, the parasite is targeted by selective host cell autophagy in vitro and in vivo (Prado et al., 2015; Thieleke-Matos et al., 2016). In addition to LC3, ubiquitin, the selective autophagy receptor p62, and lysosomes also localise to the PVM. The major difference to canonical xenophagy is that LC3 is localised in the already existing PVM and not into a newly formed double membrane. Importantly, LC3 is directly incorporated in the outer leaflet of the PVM. This was elegantly confirmed by expressing an $LC3^{G120A}$ mutant that cannot be lipidated and incorporated into membranes (Kabeya et al., 2000). This mutated LC3 did not localise to the PVM in infected cells confirming that lipidation and not interaction with, for example, other PVM proteins causes the observed recruitment (Prado et al., 2015).

In the present study, we analysed the molecular mechanism of LC3-targeting to the PVM. We used the clustered regularly interspaced palindromic repeats (CRISPR)/Cas9 nickase approach to generate gene knockouts for *FIP200* and *ATG5* in a *Plasmodium*-susceptible HeLa cell line. FIP200 is a member of the autophagy initiation complex, and ATG5 is part of the autophagy elongation machinery that processes and incorporates LC3 into the forming autophagosome membrane (Figure 1). Infection of these knockout cell lines revealed that the recruitment of LC3 to the PVM follows a noncanonical autophagy pathway, involving the elongation machinery, but not the initiation complex. Unexpectedly, the presence of LC3 at the PVM is not needed to attract lysosomes, suggesting that lysosomal recruitment in *P. berghei*-infected host cells follows an LC3-independent mechanism.

2 | RESULTS

2.1 | A functional PVM is required for LC3 incorporation

Immunofluorescence analysis revealed that host cell LC3 targets the PVM soon after infection of cells with *P. berghei*, and this labelling continues until the early schizont stage (Figure 2a). Only at the late schizont stage are LC3-positive vesicles mostly redistributed into the cytosol (Figure 2a). LC3-targeting to the PVM has also been shown

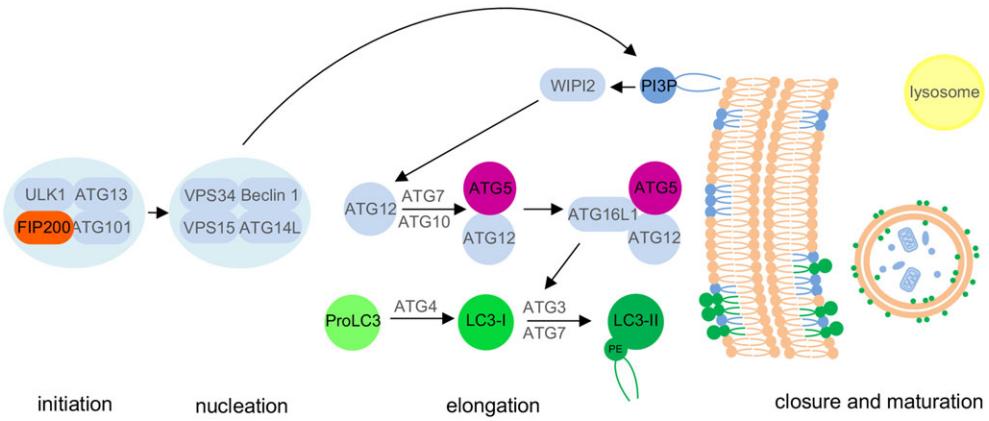

FIGURE 1 Autophagosome formation. When the initiation complex, including FIP200, is active, it regulates a class III phosphatidylinositol 3-kinase complex. Local formation of phosphatidylinositol 3-phosphate (PI(3)P) promotes phagophore formation (nucleation). Elongation of the phagophore depends on two ubiquitin-like conjugation systems. In the first, ATG12 is conjugated to ATG5 by ATG7 and ATG10. In the second, ATG7 and ATG3 mediate the conjugation of cytosolic LC3 (LC3-I) to phosphatidylethanolamine (PE) to form LC3-II, which is then incorporated into the autophagosomal membrane. Once formed, autophagosomes fuse with lysosomes, leading to degradation of their contents. In this study, we generated gene knockouts of FIP200 (orange) and ATG5 (purple) in HeLa cells. (FIP200: FAK family kinase-interacting protein of 200 kDa; PI(3)P: phosphatidylinositol 3-phosphate; ATG: autophagy-related; LC3: microtubule-associated protein 1 light chain 3 (homologue of yeast Atg8), PE: phosphatidylethanolamine)

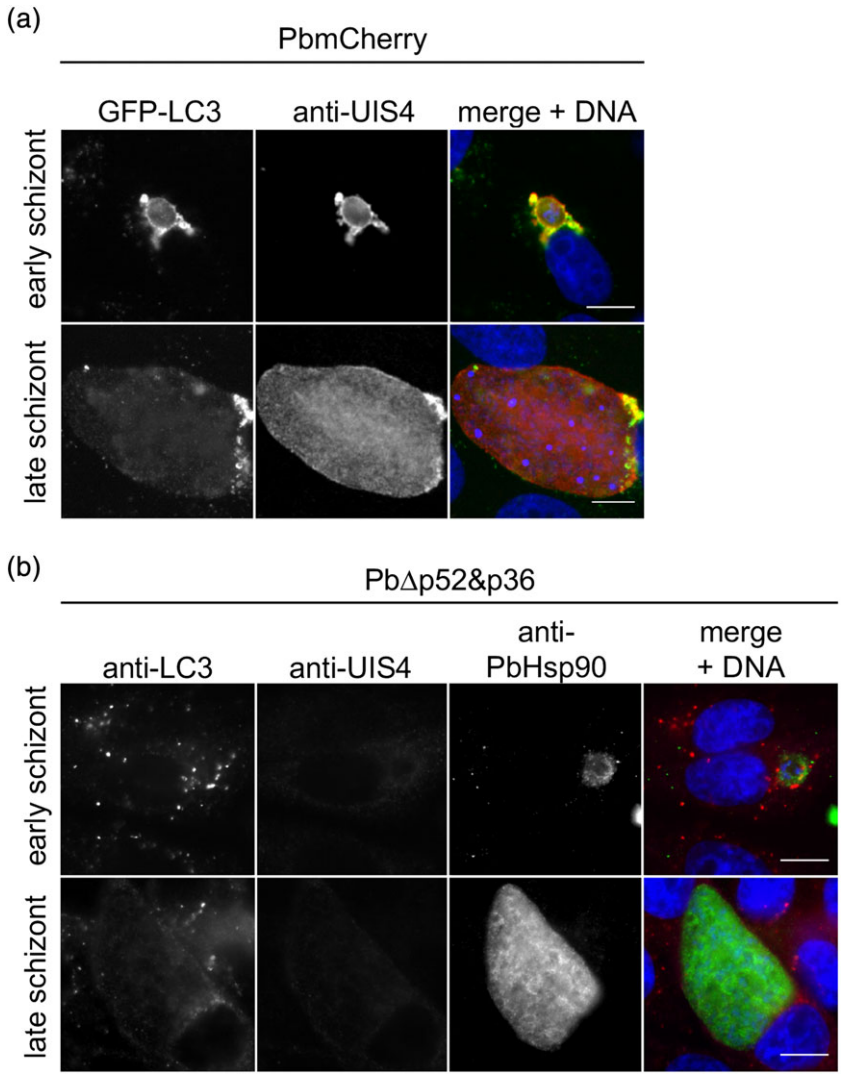

FIGURE 2 A functional PVM is required for LC3 incorporation. (a) Fully virulent parasites provoke LC3 recruitment to the PVM. GFP-LC3-expressing HeLa cells were infected with mCherry-expressing *P. berghei* parasites (PbmCherry). At early and late schizont stages, cells were fixed and stained with anti-UIS4 to label the PVM (red). DNA was labelled with DAPI (blue). Scale bars: 10 μm. (b) Parasites that are compromised in PVM formation do not recruit LC3. HeLa cells were infected with GFP-expressing *Δp52&p36 P. berghei* parasites (PbΔp52&p36) that are compromised in PVM formation. At early and late schizont stages, cells were fixed and stained with anti-LC3 (red), anti-UIS4 (far red) and anti-PbHsp90 to increase the signal of the parasite cytoplasm (green). DNA was labelled with DAPI (blue). Note that *Δp52&p36 P. berghei* parasites are negative for anti-UIS4 PVM staining and for LC3 labelling. Scale bars: 10 μm

by intravital imaging in GFP-LC3 mice, confirming that it is indeed a physiological event (Prado et al., 2015). To verify that LC3 specifically labels the PVM, we made use of *P. berghei Δp52&p36* parasites (Annoura et al., 2012; Ploemen et al., 2012), which infect host cells without the formation of a functional PVM. It has been shown previously that the vast majority of these knockout parasites (98%) abort development soon after invasion but some of them are able to complete liver stage development residing free in the cytoplasm of the host cell (Ploemen et al., 2012). Infection of HeLa cells with these parasites (Figure 2b) did not result in a LC3 accumulation comparable to what is observed in the case of fully virulent control parasites (PbmCherry; Figure 2a). This implies that host cell autophagy labels specifically the PVM in *P. berghei*-infected cells, but does not recognise the parasite plasma membrane in the case of *Δp52&p36 P. berghei* parasites.

2.2 | LC3 is directly incorporated into the PVM

To determine the molecular mechanism of LC3 incorporation into the PVM, we considered two possible options: either LC3-positive autophagosomes fuse with the PVM or LC3 is processed, lipidated, and directly incorporated into the PVM. In the first case, we would expect to initially observe the generation of LC3-positive autophagosomes that are then transported to and fuse with the PVM. In the case of a direct incorporation, however, we expected that LC3 would appear in the PVM without the formation of autophagosomes beforehand. To analyse this, we used live cell microscopy of cells expressing GFP-LC3 and infected these with mCherry-expressing sporozoites. Time-lapse microscopy revealed that 20 min post-infection, LC3 was already incorporated into the PVM (Figure 3a, Movie S1). It is known that by 4 hr post-infection (hpi), the vast majority of parasites are labelled with LC3 (Prado et al., 2015). Quantification of LC3-labelling of the PVM between 30 min and 4 hpi revealed that already 60 min after infection more than half of the parasites were LC3 positive (Figure 3b). During this time, we observed neither enhanced autophagosome formation (Figure 3c) nor fusion of autophagosomes with the PVM, indicating that the source must indeed be cytoplasmic LC3-I that is directly processed, lipidated, and incorporated into the PVM.

2.3 | Recruitment of LC3 to the PVM follows a noncanonical autophagy pathway

Using *Atg5*$^{-/-}$ mouse embryonic fibroblasts (MEFs), we have previously shown that ATG5 is required for the lipidation and incorporation of LC3 into the PVM (Prado et al., 2015). Because no additional autophagosomal membrane forms around the PVM-resident parasites (Prado et al., 2015), we hypothesized that membrane initiation and

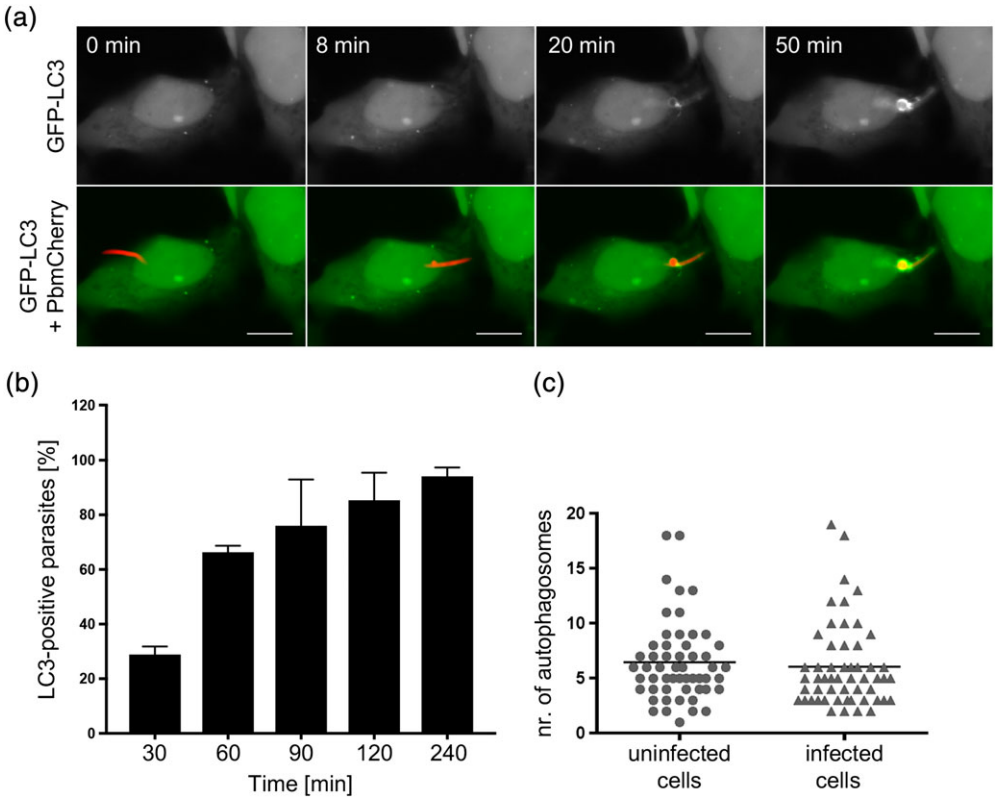

FIGURE 3 LC3 is directly incorporated into the PVM. (a) Sporozoite invasion and LC3 recruitment to the PVM. GFP-LC3-expressing HeLa cells (green) were infected with PbmCherry sporozoites (red). Time-lapse microscopy was performed during the invasion process at 30 s intervals. Still images of Movie S1 are depicted. Scale bars: 10 μm. (b) Fast LC3 recruitment to the PVM. GFP-LC3 expressing HeLa cells infected with PbmCherry sporozoites were fixed at the indicated times. An inside-outside staining was performed to distinguish intracellular from extracellular parasites. The percentage of LC3-positive intracellular parasites at each time point was determined. The graph shows mean and standard deviation of 3 independent experiments. (c) Number of autophagosomes are not different in infected and uninfected cells. At 4 hpi, the number of GFP-LC3-positive autophagosomes in uninfected and infected cells was counted and is depicted in a graph

nucleation complexes might not be needed for LC3 incorporation into the PVM. To prove this, we assessed whether the initiation complex that acts further upstream in the canonical autophagosome formation pathway is essential for LC3-incorporation into the PVM. In canonical autophagy, autophagosome formation is triggered by a initiation complex, consisting of ULK1, FIP200, ATG101, and ATG13 (Mizushima, 2010). Consistent with the induction of autophagy via the initiation complex, *Fip200*$^{-/-}$ MEFs do not form typical autophagosomes in response to starvation (Gan et al., 2006; Figure S1). We infected *Fip200*$^{-/-}$ MEFs with wildtype *P. berghei* parasites (PbWT) and monitored activation and membrane association of LC3. Despite the lack of FIP200, we still observed an incorporation of LC3 into the PVM (Figure S1). We therefore concluded that the initiation complex is not necessary for LC3 incorporation into the PVM in MEFs. However, MEFs are not ideal host cells for the parasite as within this cell type, it does not fully develop to infectious merozoites. It was therefore important to confirm this information in better suited host cells. As it has been shown that parasites can fully complete liver stage development in HeLa and HepG2 cells (Calvocalle, Moreno, Eling, & Nardin, 1994; Hollingdale, Leland, & Schwartz, 1983; Kaiser et al., 2016; Prado et al., 2015), we decided to use HeLa cells for further experiments as they can be easily genetically manipulated. In addition, they allow better microscopy analysis as they are flat and do not grow in multiple layers in culture dishes as HepG2 cells do. Firstly, we generated gene knockouts of *ATG5* and *FIP200* in HeLa cells using the CRISPR/Cas9 genetic manipulation system. To minimise the risk of off-target mutations, we used the CRISPR/Cas9 paired nickase approach, which leads to two single-strand nicks situated close to each other on the genomic DNA (Ran, Hsu, Lin, et al., 2013). ATG5 knockout was performed in GFP-LC3-expressing HeLa cells (Agop-Nersesian et al., 2017) to have a direct and easy readout assay for further analysis. FIP200 knockout was performed in WT HeLa cells. Single clones were obtained, and mutation of the respective gene loci were confirmed by sequencing of the mutated regions (Figure 4a, Table S1), by western blotting (Figure 4b,c) and by immunofluorescence analysis of starved cells and cells grown in fully supplemented medium (control; Figure 4d). In starved *ATG5*$^{-/-}$ HeLa cells, as expected, conversion of LC3-I into the lipidated LC3-II was not detected by western blotting (Figure 4b). LC3 conversion was restored upon transient expression of GFP-ATG5, in particular when cells were simultaneously starved and treated with chloroquine (CQ), which prevents lysosomal degradation and thus stops the autophagic flux (Mizushima, Yoshimori, & Levine, 2010). p62, a long-lived protein normally degraded through autophagy (Bjørkøy et al., 2005), accumulated in *ATG5*$^{-/-}$ cells. Transient addback of GFP-ATG5 was not sufficient to reverse this accumulation (Figure 4b). In contrast to WT HeLa cells, *ATG5*$^{-/-}$ cells did not exhibit formation of starvation-induced autophagosomes (Figure 4d). However, accumulations of GFP-LC3 were frequently observed in

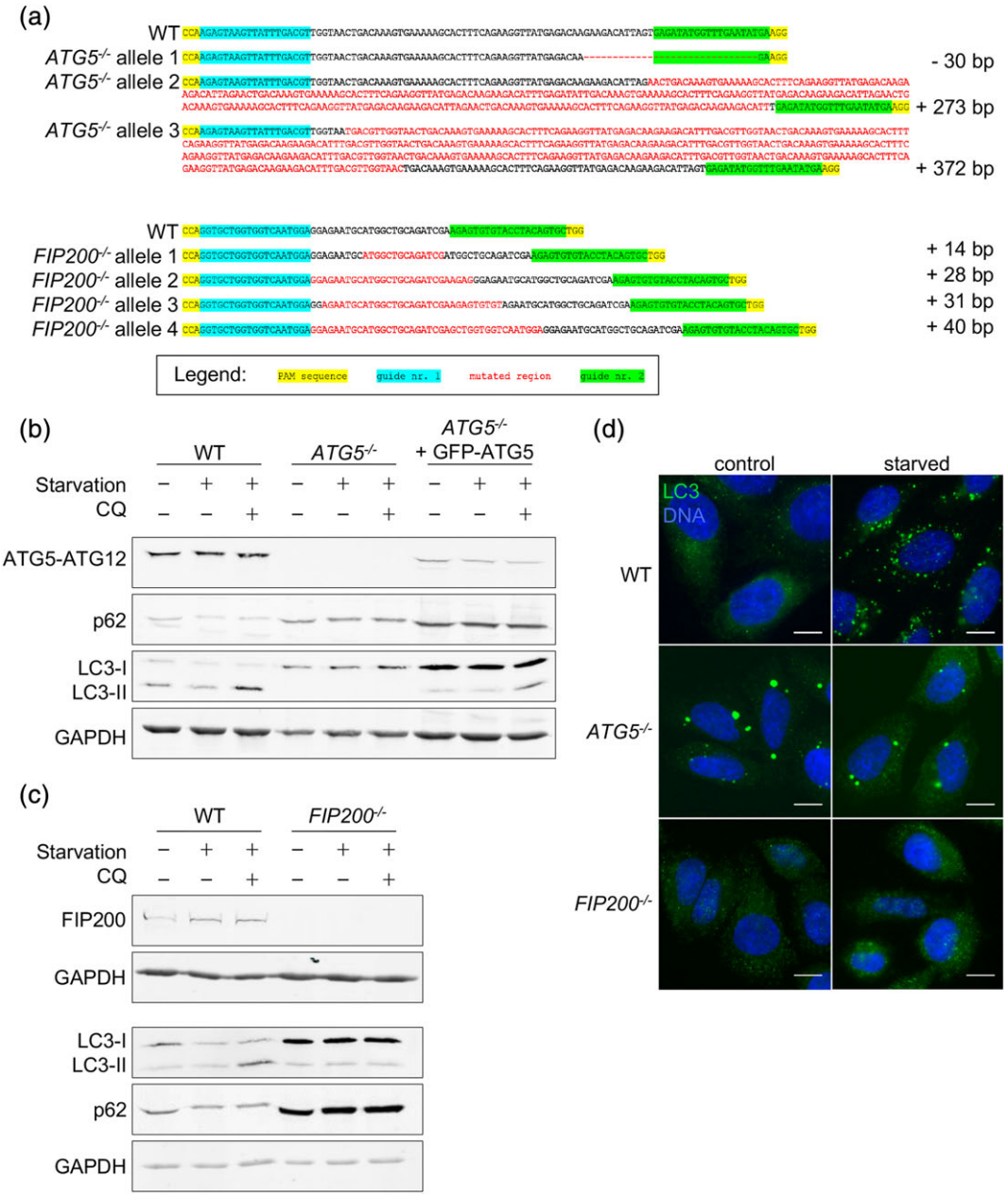

FIGURE 4 Generation of *ATG5*$^{-/-}$ and *FIP200*$^{-/-}$ cells using the CRISPR/Cas9 paired nickase approach. (a) Targeted sequence of *ATG5* and *FIP200* genomic regions. WT sequences and mutated alleles of the clones used in this study are depicted. In green and blue, the regions recognised by 2 different guideRNAs are highlighted. (b) Western blot analysis confirms knockout of *ATG5*. WT, *ATG5*$^{-/-}$, and complemented *ATG5*$^{-/-}$ HeLa cells ectopically expressing GFP-ATG5 were cultivated in growth medium or starved in EBSS with or without 10 μM chloroquine (CQ). After 2 h, cells were lysed, and western blot analysis was performed with a subsequent staining for ATG5, LC3, p62, and GAPDH as a loading control. All bands shown correspond to the endogenous proteins, except for the ectopically expressed GFP-ATG5 in lanes 7–9. (c) Western blot analysis confirms knockout of *FIP200*. WT and *FIP200*$^{-/-}$ HeLa cells were cultivated in growth medium or starved in EBSS with or without 10 μM chloroquine (CQ). After 2 h, cells were lysed, and western blot analysis was performed. For FIP200 detection, whole protein lysates were separated on an 8% SDS gel whereas for LC3 and p62 detection, RIPA protein lysates were separated on a 12% SDS gel. As a loading control, GAPDH was detected on both blots. All bands shown correspond to the endogenous proteins. (d) *ATG5*$^{-/-}$ and *FIP200*$^{-/-}$ HeLa cells are deficient in autophagosome formation. WT, *ATG5*$^{-/-}$, and *FIP200*$^{-/-}$ HeLa cells were cultivated in growth medium or starved for 2 h. Cells were fixed and stained with anti-LC3 (green) and DAPI (blue) to label DNA. Scale bars: 10 μm. Note that starvation-induced typical autophagosomes only form in WT cells

ATG5$^{-/-}$ cells. These accumulations differed clearly from autophagosomes in size and numbers and have been described before in conditions where LC3 is overexpressed (Akiko Kuma, Matsui, & Mizushima, 2007).

Western blot analysis revealed that in *FIP200*$^{-/-}$ HeLa cells, as observed before in *Fip200*$^{-/-}$ MEFs (Hara et al., 2008), conversion of LC3-I into LC3-II still occurred, but was not enhanced by starvation (Figure 4c). Not even simultaneous CQ treatment led to an accumulation of LC3-II. However, *FIP200*$^{-/-}$ cells showed overall higher levels of LC3 protein compared to wildtype HeLa cells, probably due to the reduced autophagy activity. Most likely for the same reason p62 also accumulated in *FIP200*$^{-/-}$ HeLa cells (Figure 4c). Importantly, like *ATG5*$^{-/-}$ HeLa cells, *FIP200*$^{-/-}$ cells were also unable to induce autophagosome formation upon starvation (Figure 4d).

Next, we infected *ATG5*$^{-/-}$ HeLa cells with PbmCherry sporozoites and analysed GFP-LC3 localization. Disruption of the elongation machinery by silencing of the *ATG5* gene blocked PVM labelling by LC3 (Figure 5a,c), confirming earlier observations in MEFs (Prado et al., 2015). Complementation of *ATG5*$^{-/-}$ cells with mCherry-ATG5 restored LC3-incorporation into the PVM upon infection (Figure 5a). To determine whether the autophagy initiation complex, and thus canonical autophagy, is activated to incorporate LC3 into the PVM, we next infected *FIP200*$^{-/-}$ HeLa cells with PbmCherry sporozoites. Interestingly, LC3 was still present in the PVM suggesting that the initiation complex is not necessary for LC3 incorporation into the PVM (Figure 5b,c). Since in *FIP200*$^{-/-}$ HeLa cells LC3 incorporation into the PVM was not affected, complementation experiments were not performed. Another important conclusion could be drawn from the results of this experiment: because *FIP200*$^{-/-}$ cells do not form autophagosomes, fusion of autophagosomes with the PVM cannot be a major source of PVM-associated LC3. This finding lends further evidence to our conclusion that PVM-association of LC3 is by direct recruitment from the cytoplasmic pool and not by fusion of LC3-positive vesicles with the PVM.

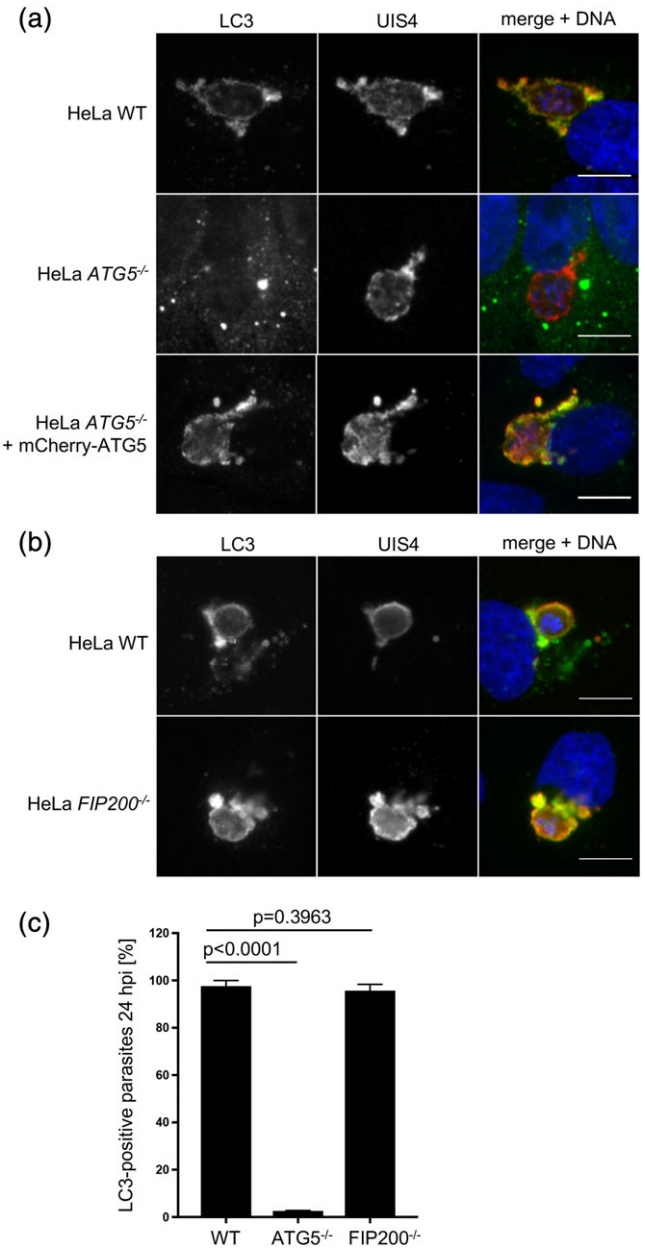

FIGURE 5 Incorporation of LC3 into the PVM in HeLa cells depends on ATG5, but not on FIP200. (a) LC3 recruitment to the PVM depends on proper processing and lipidation. WT, *ATG5*$^{-/-}$, and *ATG5*$^{-/-}$ HeLa cells complemented with mCherry-ATG5 were infected with PbmCherry sporozoites. At the early schizont stage, cells were fixed and stained with anti-LC3 (green), anti-UIS4 (red), and DAPI (blue) to label DNA. (b) LC3 recruitment to the PVM is independent of the autophagy initiation complex. WT and *FIP200*$^{-/-}$ HeLa cells were infected with PbmCherry. At the early schizont stage (24 hpi), cells were fixed and stained with anti-LC3 (green), anti-UIS4 (red), and DAPI (blue) to label DNA. Scale bars: 10 μm. (c) Quantification of LC3-labelling in infected cells (24 hpi). The graph shows mean and standard deviation of 3 independent experiments. N = 100. A student's t test was used to determine p values

In *FIP200*$^{-/-}$ HeLa cells, like in *ATG5*$^{-/-}$ HeLa cells, LC3 accumulations were detected when LC3 was overexpressed. To ensure that these are lipidation-independent protein accumulations, we simultaneously expressed RFP-LC3 and GFP-LC3^{G120A}. In WT HeLa cells, RFP-LC3, but not GFP-LC3^{G120A}, localised to autophagosomes upon starvation. In *FIP200*$^{-/-}$ cells, both forms of LC3 localised to the same accumulations, confirming that they are lipidation-independent and thus not related to canonical autophagosomes (Figure S2). We have previously shown that LC3^{G120A} is not incorporated into the *Plasmodium* PVM (Prado et al., 2015). Based on our observations in MEFs and HeLa cells, we concluded that the downstream elongation machinery, but not the initiation complex, is involved in incorporation of LC3 into the PVM. In addition, we showed that LC3 is indeed directly incorporated into the PVM and not by fusion of autophagosomes.

2.4 | Host cell autophagy has an influence on *P. berghei* liver stage development.

We have previously shown in *Atg5*$^{-/-}$ MEFs that parasites stay smaller but survive better than in WT MEFs (Prado et al., 2015). These findings suggest that impaired selective autophagy allows more parasites to develop but that they stay smaller because canonical autophagy is also impaired in *Atg5*$^{-/-}$ MEFs (Prado et al., 2015). As HeLa cells, in contrast to MEFs, allow full development of *P. berghei*, we now determined both parasite growth and parasite numbers in *ATG5*$^{-/-}$ and *FIP200*$^{-/-}$ HeLa cell lines. In both deficient cell lines, parasites were significantly smaller than in WT HeLa cells (Figure 6a). This suggests that canonical autophagy indeed provides nutrients for parasite growth. Consistent with previous results, we found more parasites in *ATG5*$^{-/-}$ cells than in WT cells (Figure 6b). This was not the case in *FIP200*$^{-/-}$ cells, suggesting that the observed selective labelling of the PVM with LC3, and most likely other autophagy proteins, can indeed contribute to parasite elimination.

2.5 | LC3 is not required to recruit lysosomes to the PVM.

In canonical autophagy, LC3-positive autophagosomes rapidly fuse with lysosomes. Inside the resulting autolysosomes, the engulfed material is degraded (Klionsky et al., 2011). For *P. berghei*-infected host cells, it has previously been shown that acidic vesicles accumulate at

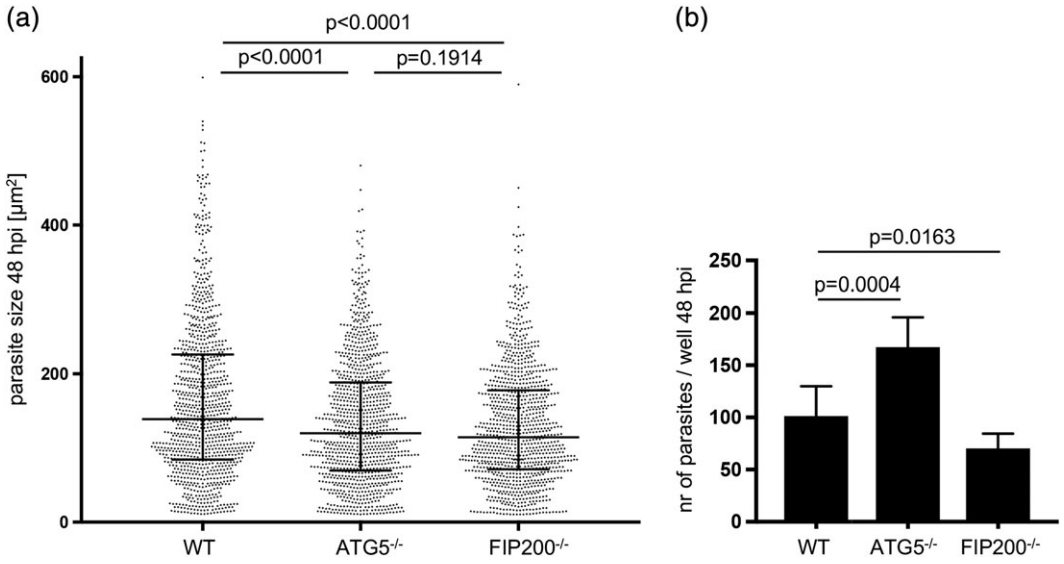

FIGURE 6 Host cell autophagy has an influence on *P. berghei* liver stage development. (a) Reduced parasite size in autophagy-deficient HeLa cells. WT, *ATG5*$^{-/-}$, and *FIP200*$^{-/-}$ HeLa cells in eight replicate wells of a 96-well plate were infected with equal numbers of PbmCherry sporozoites from the same preparation. Parasite size was determined 48 hpi using automated high throughput live cell imaging and analysis (InCell Analyzer 2000). *p* values were determined with a Mann–Whitney *U* test. The graph shows median and interquartile ranges of a representative experiment. *N* = 1,000 (b) Complete block of autophagy in ATG5-deficient HeLa cells allows more parasites to develop. Experimental setup as (a). Parasite numbers per well were determined 48 hpi. The graph shows mean and standard deviations of one representative experiment. A student's *t* test was used to determine *p* values

the PVM; however, in the vast majority of infected cells, there is no acidification of the PV (Agop-Nersesian et al., 2017; Grützke et al., 2014; Lopes da Silva et al., 2012; Prado et al., 2015; Thieleke-Matos et al., 2016). Because in *P. berghei*-infected *ATG5*$^{-/-}$ HeLa cells, LC3 was not incorporated into the PVM, we were interested whether lysosomes can still be recruited to the PVM. WT, *ATG5*$^{-/-}$, and *FIP200*$^{-/-}$ HeLa cells were infected with mCherry-expressing *P. berghei* parasites, and at the early schizont stage, the distribution of lysosomal associated membrane protein 1 (LAMP1) in infected cells was analysed. Surprisingly, we observed a similar number of parasites whose PVM was decorated with LAMP1 in infected WT and *ATG5*$^{-/-}$ Hela cells. Infected *FIP200*$^{-/-}$ HeLa cells also showed LAMP1 recruitment to the PVM (Figure 7a,b), which was expected because LC3 labelling of the PVM was not impaired in these cells. Consistent with this result, we observed a similar LAMP1 distribution in infected WT and *Atg5*$^{-/-}$ MEFs (data not shown). Lysosome association with the PVM in *P. berghei*-infected *Atg5*$^{-/-}$ MEFs has recently also been observed by Petersen et al. (2017). In conclusion, the presence of LC3 appears not to be essential for the recruitment of lysosomes to the PVM.

3 | DISCUSSION

As an intracellular pathogen, *P. berghei* is exposed to intracellular host cell defence mechanisms. This is particularly evident for attenuated *Δp52&p36 P. berghei* parasites that are compromised in PVM formation: the vast majority of these parasites are efficiently eliminated (Ploemen et al., 2012). Although living in a PV protects virulent *Plasmodium* parasites from direct exposure to such a host cell response, the host cell possesses efficient measures to even eliminate vacuole-borne pathogens. We recently showed that during the exoerythrocytic development of *P. berghei* parasites, the host hepatocyte labels the PVM with the autophagy marker protein LC3 directly after invasion (Prado et al., 2015). In this study, we provide novel insights in the molecular mechanism of this event.

Most importantly, we show that LC3-incorporation into the PVM is dependent on the autophagy elongation machinery, but not on the initiation complex and thus does not follow the canonical pathway. It is important to note that LC3 is recruited to the already existing outer leaflet of the PVM and not, as in canonical autophagy, to a newly formed double membrane structure. Similar phenomena can also be found in LC3-associated phagocytosis (LAP). LAP is a form of noncanonical autophagy that has been described in macrophages. When they take up zymosan, dead cells, or bacteria, LC3 is directly recruited to the phagosome membrane (Florey, Kim, Sandoval, Haynes, & Overholtzer, 2011; Martinez et al., 2011; Sanjuan et al., 2007). One important hallmark of LAP is that it acts independently of the initiation complex, similar to what we observed for *P. berghei*-infected host cells. Together, LC3-association with the PVM of *P. berghei*-infected host cells and LAP clearly have common features: (a) LC3 associates to the outer leaflet of a pre-existing single membrane, (b) LC3 recruitment is independent of the ULK1 initiation complex, and (c) processing and lipidation of LC3 via the elongation machinery has to occur to incorporate LC3 into the pre-existing membrane. However, in LAP, the upstream signalling events that result in LC3 recruitment are clearly defined and include generation of PI(3)P in the already existing membrane, followed by recruitment of Beclin 1. Now, it remains to be shown whether these upstream events also occur in *P. berghei*-infected cells.

Interestingly, a LAP-like elimination of the human *Plasmodium* parasite *P. vivax* during the liver stage has recently been suggested (Boonhok et al., 2016). However, despite a number of similarities, the mechanism appears to be entirely different from the observed LC3 recruitment in *P. berghei*-infected cells. Boonhok and colleagues did

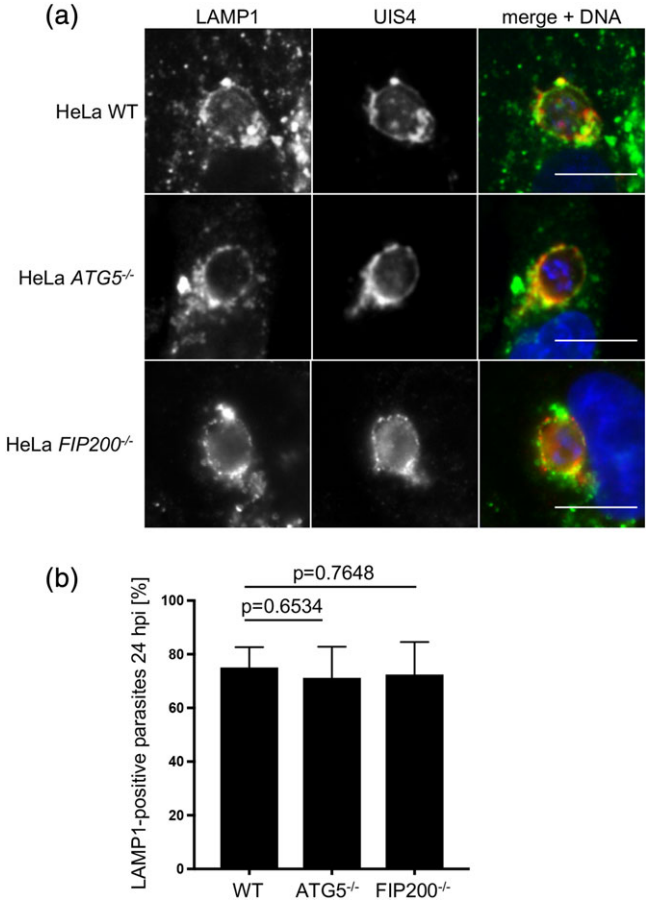

FIGURE 7 PVM-associated LC3 is not required to recruit lysosomes in HeLa cells. (a) Lysosome accumulation around parasites in WT and autophagy-deficient cells. WT and *ATG5*$^{-/-}$ HeLa cells were infected with PbmCherry parasites. At the early schizont stage, cells were fixed and stained with anti-LAMP1 (green) and anti-UIS4 (red). Representative images of LAMP1-positive parasites are shown. Scale bars: 10 µm. (b) Quantification of LAMP1-association in infected cells. The graph shows mean and standard deviation of 3 independent experiments. *N* = 100. A student's *t* test was used to determine *p* values

not observe an immediate but an induced LC3 labelling of the PVM. In contrast to *P. berghei*-infected hepatocytes, in *P. vivax*-infected cells, IFN-γ signalling is required for generation of PI(3)P, recruitment of Beclin 1, and activation of the elongation machinery followed by LC3 incorporation into the PVM. However, IFN-γ treatment induced LC3-labelling of the PVM of only around 30% of the parasites, which is considerably less than the immediate labelling of almost 100% of parasites in *P. berghei* infection. It also appears that once targeted by LC3, *P. vivax*, but not *P. berghei*, are efficiently eliminated by this intracellular immune response. In the case of *P. berghei*, a proportion of parasites escape the immediate host cell response and can complete their development (Eickel et al., 2013; Prado et al., 2015). A highly interesting and relevant aspect of this observed difference is that *P. vivax* is known to form dormant stages (called hypnozoites) in the liver, leading to relapses of the disease months to years after infection (Cogswell, 1992) whereas *P. berghei* does not form hypnozoites. An interesting hypothesis is that failure of the host cell autophagy machinery to immediately recognise *P. vivax* parasites might be the key to their persistence. Therefore, it would be very interesting to investigate how *P. vivax* hypnozoite-infected hepatocytes react to IFN-γ treatment. Another attractive scenario is that occasional PVM labelling in hypnozoite-infected hepatocytes triggers growth of the dormant forms. Because IFN-γ does not induce LC3 labelling in all infected cells, this would nicely explain why not all dormant forms are activated at the same time.

IFN-γ is also able to control host cell infection with *Toxoplasma gondii*, a parasite closely related to *Plasmodium* (Choi et al., 2014; Selleck et al., 2015). A LAP-like pathway for PVM labelling by LC3 was described in *T. gondii*-infected MEFs (Choi et al., 2014). In this pathway, the elongation machinery including ATG5 is necessary and sufficient to recruit IFN-γ inducible GTPases (IRGs). This results in the elimination of the parasite (Howard, Hunn, & Steinfeldt, 2011; Park et al., 2016). However, the autophagic response to *T. gondii* infection is known to vary between different host cell types and even parasite strains (Selleck et al., 2015), and it would not be too surprising if different *Plasmodium* species also show differences in this respect. In fact, another rodent *Plasmodium* species, *P. yoelii*, appears to provoke a slightly different LC3 recruitment to the PVM (Thieleke-Matos et al., 2016; Zhao et al., 2016). In contrast to *P. berghei*, only a proportion of parasites are immediately labelled by LC3 (Zhao et al., 2016). Only upon treatment of *P. yoelii*-infected cells with the autophagy-inducing drug rapamycin, LC3 labelling of the PVM and lysosome recruitment was observed in the majority of infected cells (Zhao et al., 2016). In summary, it appears that autophagic host cell responses vary considerably between parasite species and even parasite strains. However, in general, autophagic targeting of intracellular parasites seems to be a conserved defence strategy for infected cells.

An alternative noncanonical mechanism of LC3-incorporation into a single membrane can be triggered by osmotic imbalance. A pathway involving the vacuolar-type H^+-ATPase (V-ATPase) leads to LC3 lipidation and incorporation into endolysosomal membranes during entosis (Florey, Gammoh, Kim, Jiang, & Overholtzer, 2015). This pathway also occurs independently of the ULK1 initiation complex, but involves the autophagy elongation machinery. Interestingly, V-ATPase activity is also required for LAP, but not for LC3-incorporation into the canonical autophagosome membrane (Florey et al., 2015). A major difference to LAP is the absence of PI(3)P in the targeted membrane before LC3 recruitment. The main question for future research on LC3 incorporation into the PVM of *P. berghei*-infected hepatocytes is therefore to determine whether V-ATPase activity and PI(3)P recruitment is required. This would clarify whether the observed LC3 recruitment to the PVM is a typical LAP or rather depends on osmotic imbalance.

Interestingly, we observed lysosome recruitment to the PVM in ATG5-deficient host cells, which cannot mediate the lipidation of LC3 and other members of the Atg8 family. This suggests that the recruitment of lysosomes to the PVM occurs independently of LC3. The best-known functions of LC3 are the elongation of forming autophagosomal membranes and substrate recognition via autophagy receptors during selective autophagy (reviewed in Shpilka, Weidberg, Pietrokovski, & Elazar, 2011). These functions may not be of importance in *Plasmodium* infection or LAP, as LC3 is incorporated into a pre-existing membrane. The function of LC3 in autophagosome maturation, the process during which the autophagosome fuses with

vesicles from the endocytic pathway and eventually with lysosomes, is less clear.

LC3 is known to interact with proteins that function in autophagosome-lysosome fusion. Firstly, LC3 can interact with FYCO1 (FYVE and coiled coil domain containing 1), which in turn binds to the GTPase Rab7. Rab7, localised on the membranes of late endosomes and autophagosomes, is involved in their fusion with lysosomes (Pankiv et al., 2010). Secondly, PLEKHM1 (PLEcKstrin Homology domain containing protein family Member 1) can interact with LC3 on the autophagosomal membrane (McEwan et al., 2015). Recently, Nguyen et al. showed that in HeLa cells, Atg8 family members, especially of the GABARAP subfamily, are essential for autophagosome lysosome fusion by recruiting PLEKHM1 (Nguyen et al., 2016). PLEKHM1 recruits the HOPS complex (HOmotypic fusion and vacuole Protein Sorting) and the SNARE protein STX17 (Syntaxin 17), which are important in autophagosome–lysosome fusion (Itakura, Kishi-Itakura, & Mizushima, 2012; McEwan et al., 2015). However, it has been shown that LC3 is dispensable for autophagosome-lysosome fusion using a cell free content mixing system (Morvan et al., 2009). Studies in yeast even reported that recycling of Atg8 from the outer autophagosomal membrane could be the signal triggering autophagosome maturation, meaning that the presence of Atg8 could inhibit maturation (Nair et al., 2012; Yu et al., 2012). Interestingly, it has recently been shown that the presence of mammalian Atg8 family proteins is essential for maturation of the LAP-targeted phagosome (Martinez et al., 2015). However, also in LAP, the presence of LC3 at the phagosome membrane seems to delay recruitment of lysosomal markers (Romao et al., 2013). This is in contrast to *P. berghei* infection, where LC3, p62, and lysosomal markers often label the PVM simultaneously.

It is important to note that in *P. berghei*-infected cells, association of lysosomes with the PVM in most cases does not lead to acidification of the PV and subsequent elimination of the parasite (Prado et al., 2015). It has been proposed before that successfully developing parasites are able to restrict fusion events to vesicles that are only slightly acidic (Lopes da Silva et al., 2012). However, it is well possible that fusion of lysosomes with the PVM is simply not sufficient to establish an acidic environment due to the porous structure of the PVM. As we have shown before, many parasites can lose PVM-association of lysosomal markers, and this correlates with successful exoerythrocytic development (Prado et al., 2015). It will now be interesting to study if the parasite actively controls the presence of autophagic and lysosomal proteins at the PVM. This might shed light on events that decide on the fate of each parasite during its exoerythrocytic development, and thus on the progress of the infection.

4 | EXPERIMENTAL PROCEDURES

4.1 | Animal work statement

Mice used in the experiments were between 6 and 10 weeks of age and were bred in the central animal facility of the University of Bern. Experiments were conducted with strict accordance to the guidelines of the Swiss Tierschutzgesetz (TSchG; Animal Rights Laws) approved by local authorities in Bern.

4.2 | Culture, treatment and in vitro infection of HeLa and MEFs

HeLa cells (European Cell Culture Collection) were cultured in minimum essential medium with Earle's salts (MEM EBS; BioConcept, 1-31F01-I), supplemented with 10% FCS (GE Healthcare), 100 U penicillin, 100 µg/ml streptomycin, and 2 mM L-glutamine (all from BioConcept). Wild-type and *Atg5*$^{-/-}$ MEFs (kindly provided by N. Mizushima, University of Tokyo; Kuma et al., 2004) and wild-type and *Fip200*$^{-/-}$ MEFs (Gan et al., 2006) were maintained in Dulbecco's Modified Eagle Medium (DMEM; 1-26F01-I), supplemented with 10% FCS, 100 U penicillin, 100 µg/ml streptomycin, 2 mM L-glutamine. Cells were cultured at 37 °C and 5% CO_2 and split using Accutase (Innovative Cell Technologies) diluted 1:2 in phosphate-buffered saline (PBS; 137 mM NaCl, 2.7 mM KCl, 10 mM Na_2HPO_4, 1.8 mM KH_2PO_4, pH 7.4).

For starvation experiments, cells were rinsed 3 times with PBS and subsequently incubated in Earles Balanced Salt Solution (EBSS; Sigma, E2888) for 2 h before fixation or preparation of protein lysates. For simultaneous chloroquine treatment and starvation, the same procedure was used as with starvation, but with EBSS containing 10 µM chloroquine (Sigma-Aldrich C6628).

For infection of cells, salivary glands of infected *Anopheles stephensi* mosquitoes were isolated and disrupted to release sporozoites. Sporozoites were incubated with cells in the respective medium containing 25 µg/ml Amphotericin B (Amresco E437) for 2 hr. Subsequently, cells were washed with PBS and incubated in the respective medium containing 2.5 µg/ml Amphotericin B.

4.3 | Parasite strains

All parasite strains used have a *P. berghei* ANKA background. PbmCherry, as PbWT parasites, are phenotypically wildtype, but PbmCherry express cytosolic mCherry under the control of the *P. berghei* hsp70 regulatory sequences (Burda et al., 2015). PbΔp52&p36 parasites (line 1409 cl1) lack the expression of the P52 and P36 protein, but express the reporter protein GFP in the cytosol (Ploemen et al., 2012).

4.4 | Transfection of HeLa cells

HeLa cells were harvested by Accutase treatment, and 2×10^6 cells were pelleted by centrifugation at 1000 × g for 2 min at room temperature. They were resuspended in Nucleofector V solution (Lonza, VVCA-1003) and transfected with 1 µg of plasmid DNA using program T-28 of the Nucleofector 2b transfection device according to the manufacturer's instructions.

4.5 | Plasmids

The plasmid encoding GFP-LC3B was kindly supplied by Jonathan C. Howard, Cologne, Germany (Martens et al., 2005). The GFP-LC3^{G120A} plasmid was described before (Prado et al., 2015). Plasmids pX335-U6-Chimeric_BB-CBh-hSpCas9n(D10A) (plasmid 42335, provided by Feng Zhang; Cong et al., 2013), and mCherry-ATG5 (plasmid 13095, provided by Roberta Gottlieb; Hamacher-Brady et al., 2007) were

obtained from Addgene. To generate a plasmid encoding GFP-ATG5, the *ATG5* cassette from pmCherry-ATG5 was subcloned with XhoI and KpnI restriction sites into pcDNA3.1(-)-Puro-EGFP-C1, a kind gift from Erich Nigg, Basel, Switzerland.

4.6 | Generation of knockout cell lines

The CRISPR/Cas9 paired nickase approach described by Ran, Hsu, Lin, et al. (2013) was used to knock out the *FIP200* and *ATG5* genes. CRISPR guide RNA pairs (gRNAs) were designed to target an exon common to all relevant variants of the gene of interest. Cloning of the guideRNA sequences into the plasmid pX335-U6-Chimeric_BB-CBh-hSpCas9n(D10A), (a gift from Feng Zhang; Addgene plasmid 42335; Cong et al., 2013), was performed following the protocol of the Zhang laboratory (Ran, Hsu, Wright, et al., 2013). GuideRNAs are listed in Table S1. HeLa cells were transfected with a pair of pX335 plasmids, each encoding for one guideRNA and Cas9 nickase, and the plasmid pcDNA3.1(-)-Puro-mCherry-C1 (a gift from Erich Nigg, Basel, Switzerland). Transfection was performed following the protocol described above. Transfected cells were selected with 0.5 µg/ml Puromycin from 1 to 3 days post transfection. Thereafter, selected cells were cultivated for 10 days before being plated in 96-well plates. Single colonies were expanded and screened for the absence of the respective protein. The knockout of *ATG5* was performed in stable transfected HeLa cells, constitutively expressing GFP-LC3 (Agop-Nersesian et al., 2017), whereas *FIP200* was targeted in WT HeLa cells.

For *ATG5*$^{-/-}$ cells, the clones were first screened for the absence of LC3-II by western blotting. Later, western blotting also confirmed the absence of ATG5 in the clone used for this study. For *FIP200*$^{-/-}$ cells, the first screening step was the isolation of genomic DNA using the Quickextract™ DNA extraction solution 1.0 (Epicentre). The targeted region was amplified using PCR (PCR primers are listed in Table S1). In several clones, different amplicon lengths were detected by agarose gel electrophoresis. The clones with amplicon lengths different than that of WT cells were used for further screening by western blotting. Cells were simultaneously starved and treated with 10 µM chloroquine for 2 hr before lysis and western blotting. Clones that showed the smallest change in LC3-II/LC3-I levels upon treatment were used for further characterisation. For the *ATG5*$^{-/-}$ and *FIP200*$^{-/-}$ clones used in this study, genomic DNA was isolated, and the targeted regions were cloned into pJet1.2 (CloneJET PCR Cloning Kit, Thermo Fisher Scientific K-1232) and sequenced. Sequencing of targeted genomic regions of knockout lines confirmed the presence of DNA alterations that lead to the knockout phenotype (summarised in Table S1). In addition, western blotting and immunofluorescence analysis showed the expected behaviour after autophagy induction (Figure 4).

4.7 | Protein lysates and western blotting

Cells were seeded into 6-well plates to reach confluency the next day. Twenty-four hours later, after the appropriate treatment, cells were rinsed with PBS and lysed directly in the well for 30 min on ice with 200 µl ice-cold RIPA buffer per well (50 mM Tris-HCl pH 7.0, 1% NP-40, 0.5% Na-deoxicholate, 150 mM NaCl, 2 mM Na-F, 0.1% SDS, Complete™ Mini EDTA-free protease inhibitor cocktail; Sigma-Aldrich). Next, the lysate was centrifuged at 16,000 g/15 min/4°C. The supernatant was mixed with 5× concentrated Laemmli sample buffer (final concentration: 2% glycerol, 25 mM Tris HCl pH 6.8, 0.8% SDS, 0.004% bromophenolblue, 2% 2-mercaptoethanol). Proteins were denatured at 90 °C for 5 min. To detect FIP200, cells were rinsed with PBS and lysed directly in the well with 200 µl 95°C 1× Laemmli sample buffer. After 1 min, the lysate was collected and incubated for 5 min at 95 °C. To detect FIP200, the proteins were separated on 8% SDS PAGE. For all other proteins, 12% SDS PAGE was used. PageRuler Prestained NIR Protein Ladder (Thermo Fisher Scientific) was used as a molecular weight marker. The transfer to nitrocellulose membranes was performed in a tank blot device (Hoefer). Five percent fat free milk in TBST (Tris-buffered saline with Tween20; 10 mM Tris, 150 mM NaCl, 0.05% Tween 20) was used for blocking the membranes and antibody incubation. Antibodies used were rabbit anti-FIP200 (12436 (D10D11), Cell Signalling Technology, 1:500), rabbit anti-LC3B (L7543, Sigma-Aldrich, 1:1,500), mouse anti-p62 (M162-3, MBL international, 1:1,000), and chicken anti-GAPDH (AB2302, EMD Millipore, 1:5,000). Blocking and incubation with rabbit anti-ATG5 (2630, Cell Signalling Technology, 1:1,000) was performed in 5% Bovine Serum Albumin (BSA, Sigma-Aldrich) in TBST. For secondary antibody incubation, anti-rabbit or anti-mouse IgG 800 CW IRDye and anti-chicken or anti-mouse IgG 680 LT IRDye (Li-Cor Biosciences, both 1:10,000) were diluted in 5% milk in TBST. A Li-Cor Odyssey Imaging system (Li-Cor Biosciences) was used for detection.

4.8 | Indirect immunofluorescence analysis

After the indicated time periods, cells were fixed with 4% paraformaldehyde in PBS for 10 min at room temperature. Subsequently, they were permeabilized in 0.05% Triton X-100 (Fluka Chemie, T8787) in PBS or in 10 mg/ml digitonin (Sigma-Aldrich, D141) in PBS for the anti-LC3 antibody. After washing with PBS, unspecific binding sites were blocked by incubation in 10% FCS in PBS for 10 min at room temperature followed by incubation with primary antibody in 10% FCS in PBS. Primary antibodies were mouse anti-LC3 (MBL international, M152-3; 1:250), rabbit anti-UIS4 antiserum (provided by P. Sinnis, Baltimore, USA; 1:500), chicken anti-*P. berghei* Hsp90 (1:500; Van De Sand et al., 2005), rabbit anti-CSP (1:1,000; Rennenberg et al., 2010), rat anti-mouse-LAMP1 (Developmental Hybridoma Bank, clone 1D4B; 1:1,000), or mouse anti-human-LAMP1 (Developmental Hybridoma Bank, clone H4A3; 1:1,000). For anti-LAMP1 antibodies, 0.1% Saponin (Fluka) was added to the antibody solution. For inside-outside staining, the permeabilization step was skipped, to distinguish intracellular from extracellular parasites. Cells were fixed with 2% paraformaldehyde in PBS for 3 min at room temperature, followed directly by blocking and staining of the extracellular parasites with anti-CSP antibody. Subsequently, the cells were incubated with fluorescently labelled secondary antibodies in 10% FCS/PBS for at least 45 min using the following antibodies: anti-mouse Alexa488 (Invitrogen, A11001, 1:2,000), anti-rabbit Alexa488 (Invitrogen, A11008, 1:2,000), anti-rabbit Alexa594 (Invitrogen, A21207, 1:2,000), anti-rat Alexa488 (Invitrogen, A11006, 1:2,000), anti-rat Alexa594 (Invitrogen,

A21209, 1:2,000), and anti-rabbit Cy5 (Dianova; 1:2,000). DNA was visualised by staining with 1 μg/ml DAPI (Sigma-Aldrich) for 5 min. Labelled cells were mounted on microscope slides with Dako Fluorescent Mounting Medium (Dako, S3023) and analysed by widefield microscopy using a Leica DM5500B epifluorescence microscope. Image processing was performed using FIJI.

4.9 | Quantification of LC3 and LAMP1 association with the PVM

HeLa cells infected with *P. berghei* parasites were fixed 24 hpi and labelled with anti-LC3 or anti-LAMP1 and anti-UIS4 antibodies (see Section 4.8). One hundred infected cells were imaged per experiment and cell type. Quantification was performed visually. If the LC3 or LAMP1 signal covered more than 30% of the area surrounding the parasite, it was considered positive. Distinction was not made between weak or completely absent association. GraphPad Prism version 7 was used to draw graphs and perform statistical analyses.

4.10 | Live cell imaging and time-lapse microscopy

Live cell imaging and time-lapse microscopy were performed using a Leica DMI6000B widefield epifluorescence microscope. During imaging, cells were kept in 5% CO_2 at 37 °C. Images were acquired using a Leica HCX PL APO CS 63 × 1.2 water objective and the Leica LAS AF Software, version 2.6.0.7266. Image processing was performed using FIJI. Automated live cell imaging was used to determine parasite size and numbers. mCherry-expressing parasites were imaged with an INCell Analyser 2000 automated live cell imaging system (GE Healthcare Life Sciences). InCell Developer Toolbox 1.7 software was used to analyse the acquired images. Segmentation was done using the "object" mode in the mCherry channel, and post processing was done to exclude objects smaller than 10 μm^2. GraphPad Prism version 7 was used to draw graphs and perform statistical analyses.

ACKNOWLEDGEMENTS

We thank Rebecca R. Stanway for carefully reading this manuscript. Jonathan Howard is thanked for the GFP-LC3 plasmid, Erich Nigg for the pcDNA3.1(-)-Puro-EGFP-C1 plasmid, and Photini Sinnis for the UIS4 antiserum. We are also grateful to the MIC (Microscope Imaging Centre) in Bern for providing excellent microscopy facilities. We thank the Swiss National Science Foundation (grants 310030_159519 and 316030_145013 to VH), the SystemsX consortium (MalarX grant 51RTPO_151032 to VH), the EviMalaR EU consortium to RW and VH, and the Japan Society for the Promotion of Science (grant GR16106) for financial support to RW and TA.

AUTHORS' CONTRIBUTIONS

RW, NE, TA, JS, and LN conducted the experiments. SK, JG, and VH coordinated the project; RW, NE, JS, TA, SK, and VH analysed the data; RW, NE, TA, SK, JG, and VH conceived and designed experiments; RW, NE, and VH wrote the paper.

REFERENCE

Agop-Nersesian, C., De Niz, M., Niklaus, L., Prado, M., Eickel, N., & Heussler, V. T. (2017). Shedding of host autophagic proteins from the parasitophorous vacuolar membrane of *Plasmodium berghei*. *Scientific Reports*, *7*(2191), 1–14. https://doi.org/10.1038/s41598-017-02156-7

Annoura, T., Ploemen, I. H. J., van Schaijk, B. C. L., Sajid, M., Vos, M. W., van Gemert, G. J., … Khan, S. M. (2012). Assessing the adequacy of attenuation of genetically modified malaria parasite vaccine candidates. *Vaccine*, *30*(16), 2662–2670. https://doi.org/10.1016/j.vaccine.2012.02.010

Bano, N., Romano, J. D., Jayabalasingham, B., & Coppens, I. (2007). Cellular interactions of *Plasmodium* liver stage with its host mammalian cell. *International Journal for Parasitology*, *37*, 1329–1341. https://doi.org/10.1016/j.ijpara.2007.04.005

Bjørkøy, G., Lamark, T., Brech, A., Outzen, H., Perander, M., Øvervatn, A., & Stenmark, H. (2005). p62/SQSTM1 forms protein aggregates degraded by autophagy and has a protective effect on huntingtin-induced cell death. *The Journal of Cell Biology*, *171*(4), 603–614. https://doi.org/10.1083/jcb.200507002

Boonhok, R., Rachaphaew, N., Duangmanee, A., Chobson, P., Pattaradilokrat, S., Utaisincharoen, P., … Ponpuak, M. (2016). LAP-like process as an immune mechanism downstream of IFN-γ in control of the human malaria *Plasmodium vivax* liver stage. *Proceedings of the National Academy of Sciences*, *113*(25), E3519–E3528. https://doi.org/10.1073/pnas.1525606113

Burda, P. C., Roelli, M. A., Schaffner, M., Khan, S. M., Janse, C. J., & Heussler, V. T. (2015). A *Plasmodium* phospholipase is involved in disruption of the liver stage parasitophorous vacuole membrane. *PLoS Pathogens*, *11*(3), 1–25. https://doi.org/10.1371/journal.ppat.1004760

Calvocalle, J., Moreno, A., Eling, W., & Nardin, E. (1994). In vitro development of infectious liver stages of *P. yoelii* and *P. berghei* malaria in human cell lines. *Experimental Parasitology*, *79*(3), 362–373.

Choi, J., Park, S., Biering, S. B., Selleck, E., Liu, C. Y., Zhang, X., … Virgin, H. W. (2014). The parasitophorous vacuole membrane of Toxoplasma gondii is targeted for disruption by ubiquitin-like conjugation systems of autophagy. *Immunity*, *40*(6), 924–935. https://doi.org/10.1016/j.immuni.2014.05.006

Cogswell, F. B. (1992). The hypnozoite and relapse in primate malaria. *Clinical Microbiology Reviews*, *5*(1), 26–35. https://doi.org/10.1128/CMR.5.1.26

Cong, L., Ran, F. A., Cox, D., Lin, S., Barretto, R., Habib, N., … Zhang, F. (2013). Multiplex genome engineering using CRISPR/Cas systems. *Science*, *339*(6121), 819–823. https://doi.org/10.1126/science.1231143

Deretic, V., & Levine, B. (2009). Autophagy, immunity, and microbial adaptations. *Cell Host & Microbe*, *5*(6), 527–549. https://doi.org/10.1016/j.chom.2009.05.016

Eickel, N., Kaiser, G., Prado, M., Burda, P. C., Roelli, M., Stanway, R. R., & Heussler, V. T. (2013). Features of autophagic cell death in *Plasmodium* liver-stage parasites. *Autophagy*, *9*(4), 568–580. https://doi.org/10.4161/auto.23689

Florey, O., Gammoh, N., Kim, S. E., Jiang, X., & Overholtzer, M. (2015). V-ATPase and osmotic imbalances activate endolysosomal LC3 lipidation. *Autophagy*, *11*(1), 88–99. https://doi.org/10.4161/15548627.2014.984277

Florey, O., Kim, S. E., Sandoval, C. P., Haynes, C. M., & Overholtzer, M. (2011). Autophagy machinery mediates macroendocytic processing and entotic cell death by targeting single membranes. *Nature Cell Biology*, *13*(11), 1335–1343. https://doi.org/10.1038/ncb2363

Gan, B., Peng, X., Nagy, T., Alcaraz, A., Gu, H., & Guan, J. L. (2006). Role of FIP200 in cardiac and liver development and its regulation of TNFα and TSC-mTOR signaling pathways. *Journal of Cell Biology*, *175*(1), 121–133. https://doi.org/10.1083/jcb.200604129

Grützke, J., Rindte, K., Goosmann, C., Silvie, O., Rauch, C., Heuer, D., … Ingmundson, A. (2014). The spatiotemporal dynamics and membranous features of the *Plasmodium* liver stage tubovesicular network. *Traffic*, *15*(4), 362–382. https://doi.org/10.1111/tra.12151

Hamacher-Brady, A., Brady, N. R., Logue, S. E., Sayen, M. R., Jinno, M., Kirshenbaum, L. A., … Gustafsson, Å. B. (2007). Response to myocardial ischemia/reperfusion injury involves Bnip3 and autophagy. *Cell Death and Differentiation*, *14*(1), 146–157. https://doi.org/10.1038/sj.cdd.4401936

Hara, T., Takamura, A., Kishi, C., Iemura, S. I., Natsume, T., Guan, J. L., & Mizushima, N. (2008). FIP200, a ULK-interacting protein, is required for autophagosome formation in mammalian cells. *Journal of Cell Biology*, *181*(3), 497–510. https://doi.org/10.1083/jcb.200712064

Hollingdale, M. R., Leland, P., & Schwartz, A. L. (1983). In vitro cultivation of the exoerythrocytic stage of *Plasmodium berghei* in a hepatoma cell line. *The American Journal of Tropical Medicine and Hygiene*, *32*(4), 682–684.

Howard, J. C., Hunn, J. P., & Steinfeldt, T. (2011). The IRG protein-based resistance mechanism in mice and its relation to virulence in Toxoplasma gondii. *Current Opinion in Microbiology*, *14*(4), 414–421. https://doi.org/10.1016/j.mib.2011.07.002

Itakura, E., Kishi-Itakura, C., & Mizushima, N. (2012). The hairpin-type tail-anchored SNARE syntaxin 17 targets to autophagosomes for fusion with endosomes/lysosomes. *Cell*, *151*(6), 1256–1269. https://doi.org/10.1016/j.cell.2012.11.001

Kabeya, Y., Mizushima, N., Ueno, T., Yamamoto, A., Noda, T., Kominami, E., … Yoshimori, T. (2000). LC3, a mammalian homologue of yeast Apg8p, is localized in autophagosome membranes after processing. *The EMBO Journal*, *19*(21), 5720–5728. https://doi.org/10.1093/emboj/19.21.5720

Kaiser, G., De Niz, M., Zuber, B., Burda, P.-C., Kornmann, B., Heussler, V. T., & Stanway, R. R. (2016). High resolution microscopy reveals an unusual architecture of the *Plasmodium berghei* endoplasmic reticulum. *Molecular Microbiology*, *in press*, 1–17. https://doi.org/10.1111/mmi.13490

Klionsky, D. J., Baehrecke, E. H., Brumell, J. H., Chu, C. T., Codogno, P., Cuervo, A. M., … Tooze, S. A. (2011). A comprehensive glossary of autophagy-related molecules and processes (2nd edition). *Autophagy*, *7*(11), 1273–1294. https://doi.org/10.4161/auto.7.11.17661

Knodler, L. A., & Celli, J. (2011). Eating the strangers within: Host control of intracellular bacteria via xenophagy. *Cellular Microbiology*, *13*(9), 1319–1327. https://doi.org/10.1111/j.1462-5822.2011.01632.x

Kuma, A., Hatano, M., Matsui, M., Yamamoto, A., Nakaya, H., Yoshimori, T., … Mizushima, N. (2004). The role of autophagy during the early neonatal starvation period. *Nature*, *432*(7020), 1032–1036. https://doi.org/10.1038/nature03029

Kuma, A., Matsui, M., & Mizushima, N. (2007). LC3, an autophagosome marker, can be incorporated into protein aggregates independent of autophagy: Caution in the interpretation of LC3 localization. *Autophagy*, *3*(4), 323–328. https://doi.org/10.4161/auto.4012

Levine, B., Mizushima, N., & Virgin, H. W. (2011). Autophagy in immunity and inflammation. *Nature*, *469*(7330), 323–335. https://doi.org/10.1038/nature09782

Lopes da Silva, M., Thieleke-Matos, C., Cabrita-Santos, L., Ramalho, J. S., Wavre-Shapton, S. T., Futter, C. E., … Seabra, M. C. (2012). The host endocytic pathway is essential for *Plasmodium berghei* late liver stage development. *Traffic*, *13*, 1351–1363. https://doi.org/10.1111/j.1600-0854.2012.01398.x

Martens, S., Parvanova, I., Zerrahn, J., Griffiths, G., Schell, G., Reichmann, G., & Howard, J. C. (2005). Disruption of Toxoplasma gondii parasitophorous vacuoles by the mouse p47-resistance GTPases. *PLoS Pathogens*, *1*(3), 187–201. https://doi.org/10.1371/journal.ppat.0010024

Martinez, J., Almendinger, J., Oberst, A., Ness, R., Dillon, C. P., Fitzgerald, P., … Green, D. R. (2011). Microtubule-associates protein 1 light chain 3 alpha (LC3)-associated phagocytosis is required for the efficient clearance of dead cells. *Proceedings of the National Academy of Sciences of the United States of America*, *108*(42), 17396–17401. https://doi.org/10.1073/pnas.1113421108

Martinez, J., Malireddi, R. K. S., Lu, Q., Cunha, L. D., Pelletier, S., Gingras, S., … Green, D. R. (2015). Molecular characterization of LC3-associated phagocytosis reveals distinct roles for Rubicon, NOX2 and autophagy proteins. *Nature Cell Biology*, *17*(7), 893–906. https://doi.org/10.1038/ncb3192

McEwan, D. G., Popovic, D., Gubas, A., Terawaki, S., Suzuki, H., Stadel, D., … Dikic, I. (2015). PLEKHM1 regulates autophagosome-lysosome fusion through HOPS complex and LC3/GABARAP proteins. *Molecular Cell*, *57*(1), 39–54. https://doi.org/10.1016/j.molcel.2014.11.006

Mizushima, N. (2004). Methods for monitoring autophagy. *International Journal of Biochemistry and Cell Biology*, *36*(12), 2491–2502. https://doi.org/10.1016/j.biocel.2004.02.005

Mizushima, N. (2010). The role of the Atg1/ULK1 complex in autophagy regulation. *Current Opinion in Cell Biology*, *22*(2), 132–139. https://doi.org/10.1016/j.ceb.2009.12.004

Mizushima, N., & Komatsu, M. (2011). Autophagy: Renovation of cells and tissues. *Cell*, *147*(4), 728–741. https://doi.org/10.1016/j.cell.2011.10.026

Mizushima, N., Yoshimori, T., & Levine, B. (2010). Methods in mammalian autophagy research. *Cell*, *140*(3), 313–326. https://doi.org/10.1016/j.cell.2010.01.028

Morvan, J., Köchl, R., Watson, R., Collinson, L. M., Jefferies, H. B. J., & Tooze, S. A. (2009). In vitro reconstitution of fusion between immature autophagosomes and endosomes. *Autophagy*, *5*(5), 676–689. https://doi.org/10.4161/auto.5.5.8378

Mostowy, S. (2013). Autophagy and bacterial clearance: A not so clear picture. *Cellular Microbiology*, *15*(3), 395–402. https://doi.org/10.1111/cmi.12063

Nair, U., Yen, W., Mari, M., Cao, Y., Xie, Z., Baba, M., … Klionsky, D. J. (2012). A role for Atg8-PE deconjugation in autophagosome biogenesis. *Autophagy*, *8*(5), 780–793. https://doi.org/10.4161/auto.19385

Nguyen, T. N., Padman, B. S., Usher, J., Oorschot, V., Ramm, G., & Lazarou, M. (2016). Atg8 family LC3 / GAB ARAP proteins are crucial for autophagosome—Lysosome fusion but not autophagosome formation during PINK1 / Parkin mitophagy and starvation, 1–18.

Pankiv, S., Alemu, E. A., Brech, A., Bruun, J. A., Lamark, T., Øvervatn, A., … Johansen, T. (2010). FYCO1 is a Rab7 effector that binds to LC3 and PI3P to mediate microtubule plus end—Directed vesicle transport. *Journal of Cell Biology*, *188*(2), 253–269. https://doi.org/10.1083/jcb.200907015

Park, S., Choi, J., Biering, S. B., Dominici, E., Williams, L. E., & Hwang, S. (2016). Targeting by AutophaGy proteins (TAG): Targeting of IFNG-inducible GTPases to membranes by the LC3 conjugation system of autophagy. *Autophagy*, *12*(7), 1153–1167. https://doi.org/10.1080/15548627.2016.1178447

Petersen, W., Stenzel, W., Silvie, O., Blanz, J., Saftig, P., & Parton, R. G. (2017). Sequestration of cholesterol within the host late endocytic pathway restricts liver-stage plasmodium development. *Molecular Biology of the Cell*. https://doi.org/10.1091/mbc.E16-07-0531

Ploemen, I. H. J., Croes, H. J., van Gemert, G. J. J., Wijers-Rouw, M., Hermsen, C. C., & Sauerwein, R. W. (2012). Plasmodium berghei Δp52&p36 parasites develop independent of a parasitophorous vacuole membrane in Huh-7 liver cells. *PloS One*, *7*(12). e50772. https://doi.org/10.1371/journal.pone.0050772

Prado, M., Eickel, N., De Niz, M., Heitmann, A., Agop-Nersesian, C., Wacker, R., … Heussler, V. T. (2015). Long-term live imaging reveals cytosolic immune responses of host hepatocytes against plasmodium infection and parasite escape mechanisms. *Autophagy*, *11*(9), 1561–1579. https://doi.org/10.1080/15548627.2015.1067361

Ran, F. A., Hsu, P. D., Lin, C. Y., Gootenberg, J. S., Konermann, S., Trevino, A. E., … Zhang, F. (2013). Double nicking by RNA-guided CRISPR cas9 for enhanced genome editing specificity. *Cell*, *154*(6), 1380–1389. https://doi.org/10.1016/j.cell.2013.08.021

Ran, F. A., Hsu, P. D., Wright, J., Agarwala, V., Scott, D. A., & Zhang, F. (2013). Genome engineering using the CRISPR-Cas9 system. *Nature Protocols*, *8*(11), 2281–2308. https://doi.org/10.1038/nprot.2013.143\rhttp://www.nature.com/nprot/journal/v8/n11/abs/nprot.2013.143.html#supplementary-information

Rennenberg, A., Lehmann, C., Heitmann, A., Witt, T., Hansen, G., Deschermeier, C., … Heussler, V. T. (2010). Exoerythrocytic plasmodium parasites secrete a cysteine protease inhibitor involved in sporozoite invasion and capable of blocking cell death of host hepatocytes. *PLoS Pathogens*, *6*(3). https://doi.org/10.1371/journal.ppat.1000825

Romao, S., Gasser, N., Becker, A. C., Guhl, B., Bajagic, M., Vanoaica, D., … Münz, C. (2013). Autophagy proteins stabilize pathogen-containing phagosomes for prolonged MHC II antigen processing. *Journal of Cell Biology*, *203*(5), 757–766. https://doi.org/10.1083/jcb.201308173

Sanjuan, M. A., Dillon, C. P., Tait, S. W. G., Moshiach, S., Dorsey, F., Connell, S., … Green, D. R. (2007). Toll-like receptor signalling in macrophages links the autophagy pathway to phagocytosis. *Nature*, *450*(7173), 1253–1257. https://doi.org/10.1038/nature06421

Selleck, E. M., Orchard, R. C., Lassen, K. G., Beatty, W. L., Xavier, R. J., Levine, B., … Sibley, L. D. (2015). A noncanonical autophagy pathway restricts Toxoplasma gondii growth in a strain-specific manner in IFN-γ-activated human cells. *MBio*, *6*(5), e01157–e01115. https://doi.org/10.1128/mBio.01157-15

Shpilka, T., Weidberg, H., Pietrokovski, S., & Elazar, Z. (2011). Atg8 an autophagy-related ubiquitin-like protein. *Genome Biology*, *12*(226), 0–11. https://doi.org/10.1186/gb-2011-12-7-226

Spielmann, T., Montagna, G. N., Hecht, L., & Matuschewski, K. (2012). Molecular make-up of the *Plasmodium* parasitophorous vacuolar membrane. *International Journal of Medical Microbiology*, *302*(4–5), 179–186. https://doi.org/10.1016/j.ijmm.2012.07.011

Sturm, A., Amino, R., van de Sand, C., Regen, T., Retzlaff, S., Rennenberg, A., … Heussler, V. T. (2006). Manipulation of host hepatocytes by the malaria parasite for delivery into liver sinusoids. *Science*, *313*(5791), 1287–1290. https://doi.org/10.1126/science.1129720

Thieleke-Matos, C., Lopes da Silva, M., Cabrita-Santos, L., Portal, M. D., Rodrigues, I. P., Zuzarte-Luis, V., … Seabra, M. C. (2016). Host cell autophagy contributes to *Plasmodium* liver development. *Cellular Microbiology*, *18*(3), 437–450. https://doi.org/10.1111/cmi.12524

Van De Sand, C., Horstmann, S., Schmidt, A., Sturm, A., Bolte, S., Krueger, A., … Heussler, V. T. (2005). The liver stage of *Plasmodium berghei* inhibits host cell apoptosis. *Molecular Microbiology*. https://doi.org/10.1111/j.1365-2958.2005.04888.x

World Health Organization. (2015). World malaria report 2015.

Yu, Z., Ni, T., Hong, B., Wang, H., Jiang, F., Zou, S., … Xie, Z. (2012). Dual roles of Atg8-PE deconjugation by Atg4 in autophagy. *Autophagy*, *8*(6), 883–892. https://doi.org/10.4161/auto.19652

Zhao, C., Liu, T., Zhou, T., Fu, Y., Zheng, H., Ding, Y., & Zhang, K. (2016). The rodent malaria liver stage survives in the rapamycin-induced autophagosome of infected. *Nature Publishing Group*, (November), 1–9. https://doi.org/10.1038/srep38170

SUPPORTING INFORMATION

Additional Supporting Information may be found online in the supporting information tab for this article.

How to cite this article: Wacker R, Eickel N, Schmuckli-Maurer J, et al. LC3-association with the parasitophorous vacuole membrane of *Plasmodium berghei* liver stages follows a noncanonical autophagy pathway. *Cellular Microbiology*. 2017; e12754. https://doi.org/10.1111/cmi.12754